Automatic Detection and Features Computation of Weld Defects for Radiographic Inspection

Y. Boutiche
Welding and NDT Research Centre (C.S.C.)
Image and Signal Processing Laboratory
Algiers, Algeria
y.boutiche@csc.dz

M. Halimi
Welding and NDT Research Centre (C.S.C.)
Image and Signal Processing Laboratory
Algiers, Algeria
m.halimi@csc.dz

***Abstract*— In the present paper a part of an automated vision system is introduced. It allows an assessment and features computation of weld defects on digital x-rays images. The vision system contain several steps, the primordial ones are segmentation and feature computation. The segmentation is assured by using a powerful implicit active contour called Local Binary Fitting LBF. In addition the curve is represented implicitly via binary level set function. Such representation has many advantages over the others ones especially in our context. Weld defect features are computed from the segmentation result (final binary level set). We have computed several features; they are ranked in two categories: Geometric features and Statistic features. Such features are very useful in the classification of weld defects and consequently in the radiographic inspection. To validate the implemented algorithm, experiment results on three different images are presented in this paper.**

***Index Terms*— Radiographic inspection, image segmentation, LBF model, Features computation.**

I. INTRODUCTION

In industrial radiography, the usual procedure for producing a radiograph is to have a source of penetrating (ionizing) radiation (X-rays or gamma-rays) on one side of the object to be examined and a detector of the radiation (the film) on the other side as shown in figure (1). This technique is very famous in NDT (Non Destructive Testing) techniques. The human interpretation of radiographic films is a hard and difficult task when a great number of defects are to be counted and evaluated; also several experts do not have the same opinion for a given film. For that, in this work, we propose an automated vision system for the detection and evaluation of weld defects from the digital radiographic films using deformable models.

Nowadays, Image processing is more and more introduced to automate the inspection process. Our general objective is to develop algorithms able to segment, to restore, to evaluate, and to compute features of defects in radiographic images. In this context, some works, based on image processing and analysis, have been published such as those based in density-based fuzzy [1], the ones based on neural networks [2], and those based on traditional image segmentation (morphological approach) [3][4]. The most laborious drawback of those techniques is the necessity of supplementary processing to refine the segmentation results e.g. linking of the contours points.

More recently, powerful techniques are introduced in image segmentation and restoration. They are based on theories of curves evolution, Partial Differential Equations PDE, and calculus of variation [5]. They are called snakes, active contours, or deformable models. The basic idea is: from an initial curve C which is given, to deform the curve until it surrounds the objects' boundaries, under some constraints from the image. The first active contour has emerged by Kass et al.'s work [6]. This work was followed by extensive works and multiple studies in the aim to improve the capacity of extracting and segmenting images. The key elements of deformable models are: the elaboration of functionals that govern the curve evolution, the deduction of evolution equations from the functionals and finally the implementation of those equations by appropriate methods. Note that a multiple choices of those keys are allowed: according to our wish to use variational evolution or not, we present the curve explicitly or implicitly. Also, the fidelity term to data are based contour (*edge-based models*) [7-11] or based on intensity distribution (*region-based models*) [12-19]. The very interesting property of those approach's families is that they solve two great common image-processing tasks simultaneously: image denoising or restoration and image segmentation.

In the present paper we detail essentially two points: the extraction of weld defects then the computation of their geometric and statistical features. For the first step, segmentation, we have exploited the implicit *Local Binary Fitting* LBF model that is ranked in region-based models. It is based on computing locally the statistical information of the image information via the Gaussian Kernel function. Such propriety gives the model the ability to deal with an inhomogeneous intensity distribution, which is the case for almost radiographic images. The second step consists to use the segmentation results to compute many features of the extracted defect.

The rest of the present paper is structured as follows: in section 2 we discuss the proposed software vision system with

its global diagram. In section 3, we focus on the segmentation algorithm which is the LBF model. Its implementation via binary level set is the aim of section 4. Section 5 details all the steps of the proposed vision-system and the different features computed followed by the experiments results on radiographic images. We finish by a conclusion and future work.

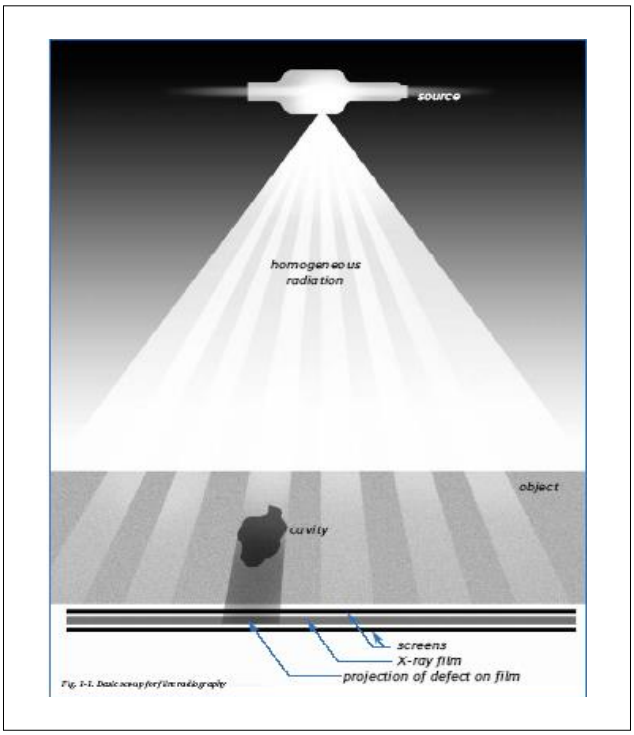

Fig. 1. Industrial radiography image forming technique [26].

II. The Proposed Vision System

In welding, the ensuring of the quality of welded joints is unavailable, for that many controls and tests are required after the visual inspection. The interpretation of radiographs takes place in three basic steps: (1) detection, (2) interpretation, and (3) evaluation. Two famous techniques are often used *X-Ray Inspection* and *Ultrasonic Inspection*. Radiographic inspection is the task that allows the detection and classification of the defects that appear on films. The classification has the goal to class and to rank welding defects: defects due to manufacture, such as lacks of fusion, slag inclusions, or welding defects due to material such as hot cracks, cavities with weld metal.

The aim of this present work is to give a computer-aided to the inspectors. Such goal is assured by the automatization of some tasks in the interpretation of radiographic films.

We display on figure (2) the main steps of the proposed vision system. Generally, captured weld radiographic images have large dimension and contain unused information , for that we have proposed the step of selecting the part of interest (ROI), this selection allows to achieve better segmentation result and computational time economy. In the following sections, we detail the two steps of the algorithm that are segmentation and features computation. The classification step is beyond this present work.

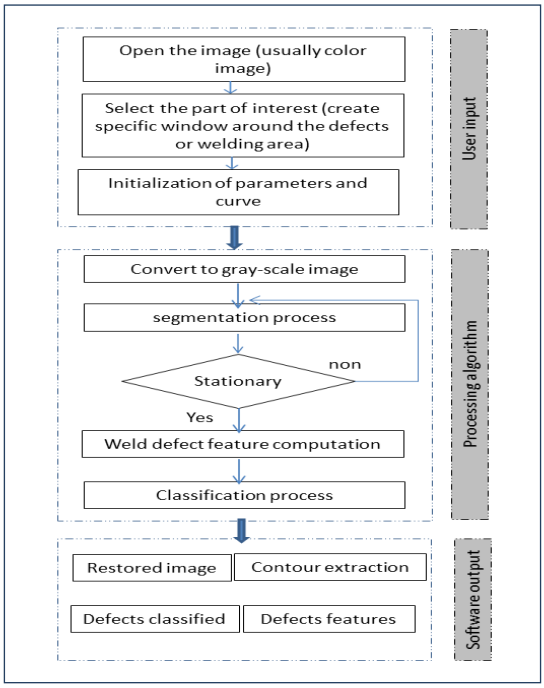

Fig. 2. Global block diagram of the main algorithms.

III. Segmentation via Local Binary Fitting Model *LBF*

Recently, region-based segmentation has been efficiently improved by introducing LBF model. C. Li et al. [20][21] proposed a model based on approximating locally the image intensities inside and outside curve. The energy functional is defined as follows:

$$E^{LBF}(C, f_1, f_2) = \lambda_1 \int_{in(C)} K_\sigma(x-y)|u_0(y) - f_1(x)|^2 dy + \lambda_2 \int_{out(C)} K_\sigma(x-y)|u_0(y) - f_2(x)|^2 dy \quad (1)$$

where x and y are points of image, σ, λ_1, and λ_2 are positive constants, K_σ is a Gaussian kernel which is a weighting function with a localization property. $f_1(x)$ and $f_2(x)$ are the two numbers that fit image intensities near the center point x. As it is known the Gaussian kernel $K_\sigma(x-y)$ takes large values at the points y near the center point x, and radically decreases to 0 as y goes away from x ($K_\sigma(x-y) \to 0$)when $|x-y| \to \infty$). However, the value of $f_1(x)$ and $f_2(x)$ for each point x are dominated by the image intensities near the center point x.

The functional $E^{LBF}(C, f_1, f_2)$in equation (1) is rewritten via Level set function as:

$$E^{LBF}(f_1, f_2, \Phi) = \lambda \int \left[\int K_\sigma(x-y) \left| u_0(y) - {}_1(x) \right|^2 H_\varepsilon(\Phi(y)) dy \right] dx + \lambda \int \left[\int K_\sigma(x-y) |u_0(y) - f_2(x)|^2 (1 - H_\varepsilon(\Phi(y))) dy \right] dx \quad (2)$$

where H is the Heaviside function. Its regularized formulation is given by equation (3) and its derivative by equation (4).

$$H_\varepsilon(z) = \frac{1}{2}\left[1 + \frac{2}{\pi} arctan\left(\frac{z}{\varepsilon}\right)\right] \quad (3)$$

$$\delta_\varepsilon(z) = \frac{1}{\pi} \frac{\varepsilon}{\varepsilon^2 + z^2}; \qquad z \in \Re \quad (4)$$

The functional in equation (2) needs to be improved in order to ensure stable evolution of level set function. For that, and inspired from the work published by Li et al. [10], the authors add the distance regularizing term to penalize the deviation of the level set function from a signed function. This term is characterized by the following integral:

$$D(\Phi) = \int_\Omega \frac{1}{2} (|\nabla \Phi(x)| - 1)^2 \, dx \quad (5)$$

Another term is necessary to regularize the zero level set contour. This one is formulated as follows:

$$L(\Phi) = \int_\Omega \delta(\Phi(x)) \, |\nabla \Phi(x)| \, dx \quad (6)$$

The final functional of LBF model to be minimized is the addition of the three integrals

$$F^{LBF}(f_1, f_2, \Phi) = E^{LBF}(f_1, f_2, \Phi) + \beta D(\Phi) + \nu L_\varepsilon(\Phi) \quad (7)$$

where β and ν are positive constant that adjust each integral. This functional should be minimized to resolve two great problems: contour extraction and image restoration.

As almost all deformable models (active contours) the minimization is ensured by gradient descent method. Based on calculus of variation [5] we compute the Euler-Lagrange equations that minimize $F^{LBF}(f_1, f_2, \Phi)$. For fixed level set Φ the $f_1(x)$ and $f_2(x)$ that minimize (7) satisfy the following equations:

$$\int K_\sigma(x-y) H_\varepsilon(\Phi(y)) (u_0(y) - f_1(x)) dy = 0$$

$$\int K_\sigma(x-y)(1 - H_\varepsilon(\Phi(y)))(u_0(y) - f_2(x)) dy = 0$$

By development and putting out the term independent from integral, we get the formulation of $f_1(x)$ and $f_2(x)$

$$f_1(x) = \frac{K_\sigma(x) * [H_\varepsilon(\Phi(x)) \, u_0(x)]}{K_\sigma(x) * [H_\varepsilon(\Phi(x))]} \quad (8)$$

$$f_2(x) = \frac{K_\sigma(x) * [(1 - H_\varepsilon(\Phi(x))) \, u_0(x)]}{K_\sigma(x) * [1 - H_\varepsilon(\Phi(x))]} \quad (9)$$

Now we keep $f_1(x)$ and $f_2(x)$ fixed and we compute the Euler-Lagrange equation that allows the update of level set function

$$\frac{\partial \Phi}{\partial t} = -\delta_\varepsilon(\Phi)(\lambda_1 e_1 - \lambda_2 e_2) + \nu \, \delta_\varepsilon(\Phi) \, \mathrm{div}\left(\frac{\nabla \Phi}{|\nabla \Phi|}\right) + \beta\left(\nabla^2 \Phi - \mathrm{div}\left(\frac{\nabla \Phi}{|\nabla \Phi|}\right)\right) \quad (10)$$

where e_1 and e_2 are given by :

$$e_1(x) = \int_\Omega K_\sigma(x-y) |u_0(x) - f_1(y)|^2 dy$$

$$e_2(x) = \int_\sigma K_\sigma(x-y) |u_0(x) - f_2(y)|^2 dy$$

These two equations should be developed to get:

$$e_1(x) = u_0^2(x)(1 * K_\sigma) - 2u_0(f_1 * K_\sigma) + (f_1^2 * K_\sigma) \quad (11)$$

$$e_2(x) = u_0^2(x)(1 * K_\sigma) - 2u_0(f_2 * K_\sigma) + (f_2^2 * K_\sigma) \quad (12)$$

so

$$\lambda_1 e_1 - \lambda_2 e_2 = (\lambda_1 - \lambda_2) u_0^2(x)[K_\sigma * 1] - 2u_0(x)[K_\sigma * (\lambda_1 f_1 - \lambda_2 f_2)] + K_\sigma * (\lambda_1 f_1^2 - \lambda_2 f_2^2) \quad (13)$$

The convolution term $K_\sigma * 1$ of equation (13) should be computed only once before the iteration. However, the other two convolution terms must be computed in each iteration.

IV. Implementation of Segmentation Algorithm

A. Level set initialization

The curve is represented implicitly via function called Binary Level set, which is defined by:

$$\Phi(x, t=0) = \begin{cases} +\rho, & x \in \Omega_0 \\ -\rho, & x \in (\Omega - \Omega_0) \end{cases} \quad (14)$$

where Ω_0 is the definition domain inside the curve. Such function has many advantages compared to the classical signed distance function, such as it is efficient and easier to construct practically, and the initial contour can take any shape [22].

B. Algorithm

As it is undermentioned above, the functional is minimized by an alternative procedure: for each iteration n and its corresponding level set Φ^n we compute f_1^n ,f_2^n followed by updating Φ^n to Φ^{n+1}. The implemented algorithm is summarized as follows:

Step 1: Initialization of parameters and curve;
Step 2: Compute the initial binary level set;
Step 3: Compute f_1^n and f_2^n;
Step 4: Update $\Phi^{n+1} = \Phi^n + \Delta t$ Energy,
where Energy is the right hand of equation (10);
Step 5: check whether the evolution is stationary,
if yes go to end, else $n = n + 1$ and return to step 3.

V. Weld Radiographic Images Segmentation and Features Computation

Our team deals with industrial radiographic images that are complex and have mediocre quality, because of the conditions

on which they have been taken. In the present work, our objective is the extraction of weld defects in order to compute their features. To achieve this goal, many steps are necessary as the diagram of fig. (2) reveals. In the following subsections we detail the main steps.

A. Selection of the region of interest ROI

More often, rough weld radiographic images are characterized by great dimension, very complex background, noisy and low contrast. Also generally those images contain some information about the material and its location. However a step of selecting region of interest (ROI) from the rough image is necessary; such selection allows to:

- Reduce time of computation;
- Avoid the processing of complex background which can be the cause of a failure contours extraction of welding defect;
- Deduct some features directly from the final segmentation outcomes.

B. Segmentation and restoration via LBF model

We have implemented the LBF model via an implicit representation of active contour using Binary Level Set function (BLS). Such representation has many advantages over the explicit one. It is able to handle sharp corners and cusps in the propagating solution, as well as topological changes. In addition, BLS is defined in the grid image which ensures the continuity of the extracted contours. However, in our context, the weld features calculated from the segmentation results will have the accuracy of a pixel. We have two possibilities to initialize the contour. First one is automatic to avoid the intervention of user twice (to select part of interest and to initial contour). The second one is done manually by using the mouse. Furthermore, we have used backward discretization scheme to approximate the temporal derivative

$$\frac{\partial \Phi}{\partial t} = \frac{\Phi^{n+1} - \Phi^{n}}{\Delta t}$$

and central derivative to compute special derivatives

$$\frac{\partial \Phi}{\partial x} = \frac{\Phi_{i+1,j} - \Phi_{i-1,j}}{2\mathrm{h}}$$

$$\frac{\partial \Phi}{\partial y} = \frac{\Phi_{i,j+1} - \Phi_{i,j-1}}{2\mathrm{h}}$$

where Δt is time step, and $\mathrm{h} = \Delta x = \Delta y$ is the space step.

The LBF functional is iterated until the number of iteration which is variable depends on the treated image. Note that, for all experiments, we have fixed the parameters to: $\lambda_1 = \lambda_2 = 1$, $\varepsilon = 1$, $\nu = 0.001 \times 255^2$, $\Delta t = 0.1$, $\beta = 1$, $h = 1$.

C. Features Computation

The computation of weld defect features is very helpful for their classification. For example, the value of roundness called also compactness that is included in $[0, 1]$ give an idea about the kind of defect. If it has little value, so the defect has sharp shape, consequently it is a crack or a lack of fusion. Contrary if roundness has large value (near 1), the defect has round shape such as porosity or inclusion [23].

Once the segmentation is achieved, we have used its outcome to compute several features. They are classed in two classes as follows:

- ***Geometric features***: geometric features are: the area, perimeter, breadth, length, centroid, roundness, equivalent diameter.
- Statistic features: this family contains information about the gray scale of defect; such as the maximum intensity, mean intensity, minimum intensity, variance, standard deviation and Weighted Centroid.

1) *Geometric features:* Using the final binary level set getting from the segmentation step, without needing to any binarisation step, we compute all the geometric features as following [24][25]:

- **Area *A***: The area of defect is given as follows:

$$A = \int H(\Phi) dx\, dy$$

which is also the total number of pixels where $\Phi = +\rho$.

$$\sum_{i,j} (i,j) \mid \Phi(\mathrm{i},\mathrm{j}) = +\rho$$

where ρ is a constant defined in equation (14).

- **Perimeter *P***: the perimeter is simply given by:

$$P = \int |\nabla H(\Phi)| dxdy$$

It is approximated numerically as follows:

$$P = \sum_{i,j} \sqrt{\left(H(\Phi_{i+1,j}) - H(\Phi_{i,j})\right)^2 + \left(H(\Phi_{i,j+1}) - H(\Phi_{i,j})\right)^2}$$

- **Breadth *B* and Length *L*:** we get *B* and *L* using, simply, the two formulas:

$$L = \max X - \min X$$

$$B = \max Y - \min Y$$

where X and Y are the vector coordinates of border pixels.

- **Centroid *C***: Centroid of the extracted object is the pixels coordinates mean of the extracted region. So $(X_{region}, Y_{region}) = (i,j) \in \Omega_0$

$$C = \left[mean(X_{region}), mean(Y_{region})\right]$$

- **Orientation ∝:** Scalar that represents the angle (in degrees ranging from -90 to 90 degrees) between the *x*-axis and the major axis of the ellipse which surrounds the region.

- **Roundness *R*:** Roundness of an object can be determined by using the formula:

$$R = \frac{4\,A\,\pi}{P^2}$$

Remark: If the Roundness is greater than 0.90 then, the object is circular in shape.

- **Equivalent Diameter *ED*:** The used formula is given by:

$$ED = \sqrt{\frac{4\,A}{\pi}}$$

2) *Statistical features:* Statistic features are related to the grey scale of the segmented region (weld). However we get back the segmented region with its original grey scale by multiplying the final binary level set by the ROI image, let's call it "GSImg" as they are displayed on (e) of figures (3), (4) and (5). From the image (GSImg), we compute the following statistical features:

- **Maximum, Minimum and Mean intensity:** Scalars specifying the value of the pixel with the greatest, lowest, and mean of the intensity in the region (weld defect).
- **Variance *V***:

$$V = mean(GSImg^2) - \left(mean(GSImg)\right)^2 \mid GSImg(i,j) \neq 0$$

- **Standard deviation**: Standard deviation is the square root of the variance.

$$\sigma = \sqrt{V}$$

- **Weighted Centroid *WC***: Weighted Centroid is computed as the simple Centroid but with taking into account the greyscale of each pixel.

The following figures display the experimental results, where three different x-rays images are the input data. On each figure we show the rough x-rays image on which the user selects the weld defect (ROI region). The second one presents the ROI image with the initial contour (dashed green line) and the curve after convergence (solid blue line). We present also the extracted contour on (c), the restored weld defect on (d), and the "GSImg" image on (e).

For the first experiment the initialization curve is automatic, on the two last experiments the user initializes the curve by using the mouse. Note that the time of the convergence of the curve depends on its initialization (location), and the computation of features depends on the segmentation results. For this reasons we must ensure that the evolution becomes stationary. On tables I and II, we have pointed out the results of all the features discussed above.

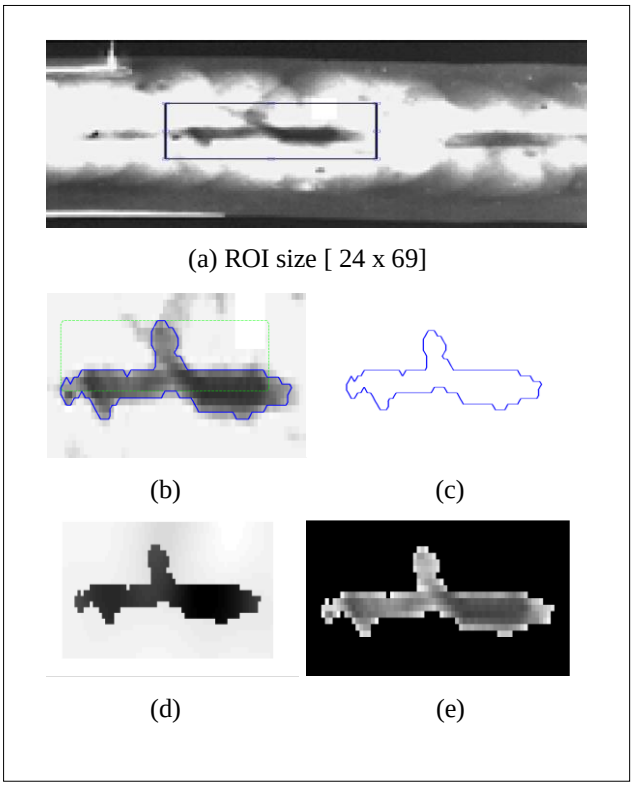

Fig. 3. Weld defect segmentation and restoration from rough radiographic image: (a) Defined ROI in rough weld radiographic image, (b) ROI image with initial contour (dashed green line) and final contour (solid blue line), (c) Edge defect, (d) restored weld defect, (e) Weld defect with its initial grey scale. $\sigma = 5$, $iteration = 250$, $CPE\ time = 2.82\ s$.

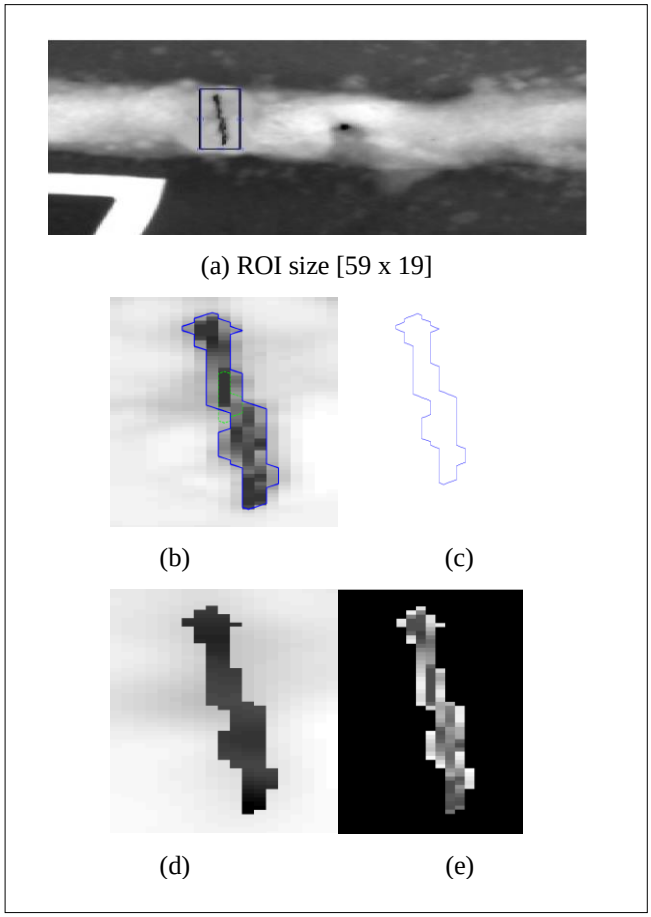

Fig. 4. Weld defect segmentation and restoration from the second rough radiographic image: (a) Defined ROI in rough weld radiographic image, (b) ROI image with initial contour (dashed green line) and final contour (solid blue line), (c) Edge defect, (d) restored weld defect, (e) Weld defect with its initial grey scale. σ=3, iteration=1900, CPE time=12.78s.

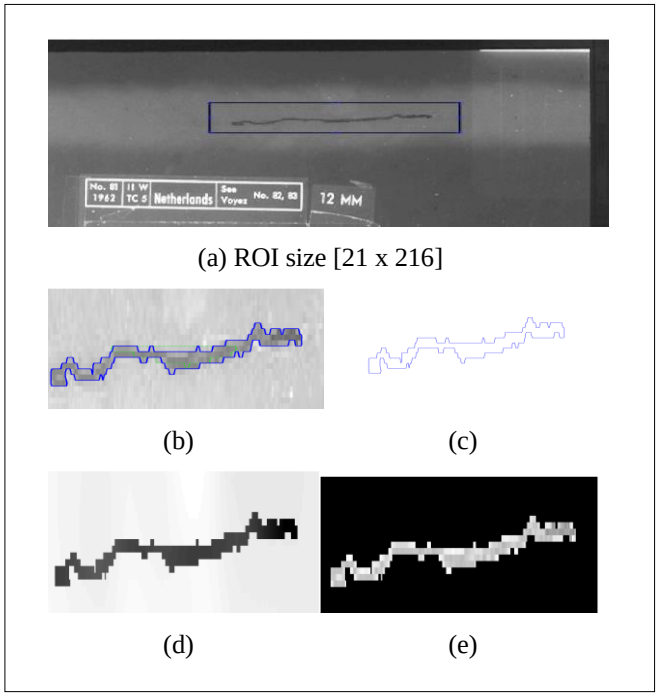

Fig. 5. Weld defect segmentation and restoration from rough radiographic image: (a) Defined ROI in rough weld radiographic image, (b) ROI image with initial contour (dashed green line) and final contour (solid blue line), (c) Edge defect, (d) restored weld defect, (e) Weld defect with its initial grey scale. σ=3, iteration=1000, CPE time=2.82 s.

TABLE I. GEOMETRIC FEATURES OF THE THREE EXTRACTED WELDS IN ABOVE EXPERIMENTS

	Area	Perimeter	Breadth	Length	Orientation	Centroid	Roundness	EquivDiameter
First exp.	338	317.25	61	14	-1.46	[36, 13]	0.042	20.74
Second exp.	146	231.79	8	50	-84.40	[11, 29]	0.034	13.63
Third exp.	477	850.50	191	11	2.03	[105, 12]	0.008	24.64

TABLE II. STATISTIC FEATURES OF THE THREE EXTRACTED WELDS IN ABOVE EXPERIMENTS

	Max Intensity	Min Intensity	Mean Intensity	Weighted Centroid	Variance	Standard deviation
First exp.	183	38	98.93	[34, 13]	0.022	0.149
Second exp.	119	26	69.01	[11, 29]	0.022	0.149
Third exp.	95	47	76.79	[104, 12]	0.005	0.072

VI. CONCLUSION

Radiography is the most common method for NDT. It is used widely for weld testing. The radiographic inspection needs several information to be elaborated; the main ones are weld defects features, and their classification. In this paper we have proposed part of the global vision-system able to help the inspectors. We have used region-based implicit active contour to achieve the extraction and restoration of defects. Even though the segmentation using deformable models are extensively studied and widely used in different domains, some difficulties and problems are always present an open subjects and real challenge for the image processing community, eg. the sensitivity to the initialization. This work needs to be completed by an algorithm of classification.

REFERENCES

[1] P. R. Reza Hasanzadeh, A. H. Rezaiea, S. H. Sadeghia, M. H. Moradi, M. Ahmadic, *A density-based fuzzy clustering technique for non-destructive detection of defects in materials*, NDT E International 40, pp. 337-346, February 2007.

[2] A. Kehoe, *The detection and evaluation of defects in industrial images*, PhD Thesis, University of Surrey, 1990.

[3] A. Laknanda, R.S. Anand, P.Kumar, *Flaw detection in radiographic weld images using morphological approach*, NDT E International 39 pp. 29-33, 2006.

[4] A. Laknanda, R.S.Anand, P. Kumar, *Flaw detection in radiographic weldment images using morphological watershed segmentation technique*, NDT E International vol. 42 pp. 2- 8, 2009.

[5] G. Aubert and P. Kornprobst : *Mathematical Problems in Image Processing Partial Differential Equations and the Calculus Of Variations*, Applied Mathematical Sciences 147, Springer Science + Business Media, LLC, New York, USA,ISBN-10: 0-387-32200-0, 2006.

[6] M. Kass, A. Witkin, D. Terzopoulos, *Snakes: active contour models*, International Journal of Computer Vision 1, 321-331, 1988.

[7] V. Caselles , R. Kimmel, G. Sapiro, *Geodesic active contours*, International Journal of Computer Vision 22 (1) 61-79, 1997.

[8] N. Paragios , R. Deriche, *Geodesic active contours and level sets for detection and tracking of moving objects*, IEEE Transaction on Pattern Analysis and Machine Intelligence 22 1-15, 2000.

[9] A. Vasilevskiy, K. Siddiqi, *Flux-maximizing geometric flows*, IEEE Transaction on Pattern Analysis and Machine Intelligence 24, 1565-1578, 2002.

[10] C. M. Li, C. Y. Xu, C.F. Gui, M.D. Fox: *Level set evolution without re-initialization: a new variational formulation*, IEEE Conference on Computer Vision and Pattern Recognition, San Diego, pp. 430-436, 2005.

[11] G. P. Zhu, Sh. Q. Zhang, Ch. H. Wang, *Boundary-based image segmentation using binary level set method*, SPIE OE Letters 46 (5), 2007.

[12] T. Chan, L. Vese, *Active contour without edges*, IEEE Transaction on Image Processing 10 (2) 266-277, 2001.

[13] R. Ronfard, *Region-based strategies for active contour models*, International Journal of Computer Vision 46 223-247, 2002.

[14] J. Lie, M. Lysaker, X. C. Tai, *A binary level set model and some application to Mumford-Shah image segmentation*, IEEE Transaction on Image Processing 15 1171-1181, 2006.

[15] A. Tsai, A. Yezzi, A. S. Willsky, *Curve evolution implementation of the Mumford-Shah functional for image segmentation, denoising, interpolation, and magnification*, IEEE Transaction on Image Processing 10 1169-1186. 2001.

[16] L. Vese, T. F. Chan, *A multiphase level set framework for image segmentation using the Mumford-Shah model*, International Journal of Computer Vision 50 271-293. 2002.

[17] H. Liu, Y. Chen, W. Chen, *Neighborhood aided implicit active contours*, IEEE Conference on Computer Vision and Pattern Recognition 1 841- 848, 2006.

[18] Z. Wang, B. Vemuri, *Tensor field segmentation using region based active contour model*, in Proceedings of the Eighth European Conference on Computer Vision (ECCV'04), Springer Lecture Notes in Computer Science, vol. 3024, pp. 304-315, 2004.

[19] W. Li, He Lei Arabinda Mishra, Ch. Li, *Active contours driven by local Gaussian distribution fitting energy*, Science Direct Signal Processing 89 pp. 2435-2447, 2009.

[20] C. Li , C. Kao, J.C. Gore, Z. Ding, *Minimization of region-scalable fitting energy for image segmentation*, IEEE Trans. Image Process, 17(10), pp. 1940-1949, 2008.

[21] C. Li, C. Kao, J. C. Gore, Z. Ding, *Implicit active contour driven by local binary fitting energy*, in Proceedings of IEEE conference on computer Vision and Pattern Recognition (CVPR), Washington, USA, pp. 1-7, 2007.

[22] Z. Kaihua, Z. Lei, S. Huihui, Z. Wengang, *Active contours with selective local or global segmentation A new formulation and level set method*, Image and Vision Computing 28 pp. 668-676, 2010.

[23] N. Nacereddine , L. Hamami , D. Ziou , *Statistical Tools for Weld Defect Evaluation in Radiographic Testing*, Journal of Nondestructive Testing and Ultrasonics ECNDT, p. 1-21, 2006.

[24] W. K. Pratt, *Digital Image Processing*, PIKS Inside, Third Edition. John Wiley & Sons, Inc., 2001

[25] T. Acharya and A. K. Ray, *Image Processing Principles and Applications*, Wiley Interscience, A John Wiley & Sons, mc., Publication, 2005.

[26] GE imagination at work, *Industrial Radiography: Image forming techniques*, GE Inspection Technologies, 2007. http://www.ge-mcs.com/download/x-ray/GEIT-30158EN_industrial-radiography-image-forming-techniques.pdf,